Available online at www.sciencedirect.com

ScienceDirect

Energy Procedia 35 (2013) 12 – 21

Energy Procedia

DeepWind'2013, 24-25 January, Trondheim, Norway

Laboratory Verification of the Modular Converter for a 100 kV DC Transformerless Offshore Wind Turbine Solution

Sverre Skalleberg Gjerde[a,*], Kjell Ljøkelsøy[b], Tore M. Undeland[a]

[a]*Norwegian University of Science and Technology, Dep. of Electric Power Engineering, 7491 Trondheim, Norway*

[b]*Sintef Energy Research, 7465 Trondheim, Norway*

Abstract

In this paper, an experimental verification of the control of a modular series connected voltage source converter suitable for an HVDC transformerless offshore wind turbine is presented. The test bench is built around a 45 kW special generator prototype with three stator segments. Three 20 kW voltage source converter modules were used in the series connected converter. The experimental results verified the feasibility of a modular, decoupled control system design approach which has earlier been investigated through simulations. In addition, the experimental results are compared to simulations to verify the model implemented in EMTDC/PSCAD.

Keywords: Offshore wind power, power electronic converter, transformerless, HVDC, experimental verification

1. Introduction

1.1. Background and motivation

The power rating of wind turbines increased almost exponentially from the 80s until 2003-2004 [1]. The development in size stopped, mainly due to logistics, but also visual pollution played a part in limiting the turbines to a rating of 2-4 MW. In recent years, a re-found interest in larger wind turbines has been observed in both academia and industry. An example is the NOWITECH reference turbine, which defines a basic design for a 10 MW, bottom fixed offshore turbine [2]. The background for this renewed interest in larger turbines is offshore wind power, where the limitations are not as strict as those found onshore. Additionally, the energy cost from offshore wind power is assumed to benefit from increased turbine rating [3].

*Corresponding authour, Tel: +47 735 94229
Email address: sverre.gjerde@ntnu.no (Sverre Skalleberg Gjerde)

doi:10.1016/j.egypro.2013.07.154

Table 1. Survey of research projects on transformerless turbine concepts

System	Generator	Converter	Output voltage	Gen.weight
Concept 1	Spoke wheel PMSG (SLiM)	CHB_{v1}	11 kV_{rms}	Light weight
Concept 2	PMSG multiple outputs	CHB_{v2}	6-35 kV_{rms}	N/A
Concept 3	Parallel 6 phase PMSG	CHB_{v3}	11 kV_{rms}	N/A
Concept 4	Multiple 3-phase - PMSG	Modular VSC	23.6 kV_{dc}	N/A
Concept 5	PMSG	Matrix	Design param.	Standard
Concept 6	Cable -PMSG	Diode+VSC	$\geq$ 20 kV_{rms}	High
Concept 7	Electrostatic DC	N/A	100-300 kV	Standard

This cost reduction is due to offshore operations being difficult and depending on strict weather windows. Fewer units means lower total number of operations. Consequently, costs related to installation and operation and maintenance (O&M) depends on the number of turbines as much as the total wind farm rating. However, an upscale of today's turbine technology will result in a massive increase in drive train mass. According to [4], the mass of a conventional, 3-phase 10 MW direct drive permanent magnet synchronous generator (DD-PMSG) alone will be approximately 300 tons.

Additionally, today's standard rated voltage (690 V_{rms}) would result in a cable current of 8.4 kA for a 10 MW turbine. Hence, the cables from the nacelle down the tower will be heavy, and several parallel cables would be needed. Medium voltage drives (3.3-6.9 $kV_{ll,rms}$) are considered, but still, the current will be substantial. Hence, it is suggested to locate the grid connecting transformer in the top of the tower. This adds to the already heavy nacelle, which will be reflected on the mechanical constraints put on the tower construction. Another issue with the transformer is maintenance related: an expensive offshore crane vessel would be needed for the replacement of this transformer, since it cannot be made modular. Therefore, avoiding this transformer is believed to be beneficial for the life cycle economy of offshore wind turbines.

With this as background, this work focuses on the development and analysis of a modular, series connected converter suitable for a large, 100 kV_{dc} transformerless offshore wind turbine.

1.2. Existing research on transformerless concepts

In the following section, a brief overview of the existing research projects on transformerless technologies is presented: In [5, 6], a cascade H-bridge (CHB) type converter has been integrated with a special, light weight, spoke wheel generator. The machine provides multiple single-phase, low voltage outputs. The output is rectified, and a distribution grid voltage level is synthesized by cascading the inverter modules on the AC-side. (Concept 1 in Tab.1). Concept 2 [7, 8, 9] is based on a similar idea, but with slightly different converter modules. [10] proposed a system with paralleled 6-phase PMSGs (Concept 3). The converter solution is similar to concept 1 and 2. A different approach is to make use of 3-phase AC/DC-converter modules and synthesize the higher output voltage (23.6 kV_{dc}) by series connecting the DC-buses [11](Concept 4). A patent is claimed for such a system [12]. The series connection of turbines is proposed in [13, 14] (Concept 5). A PMSG output is rectified by a reduced matrix converter and transmission voltage is achieved through series connecting the DC-side of the converters of each turbine. The concept is not transformerless, but the high frequency transformer is more compact than its standard 50 Hz counterpart.

A special converter topology is the common factor for the transformerless concepts reviewed above. However, there exists also other technologies. [15] (Concept 6) introduced a cable wound stator with high voltage directly from the generator. A complete different approach is presented by [16]: an electro static, variable-capacitance generator with a claimed potential of 100-300 kV_{dc} (Concept 7) is investigated.

1.3. Contribution of this paper

Concept 4 has earlier been identified as the most interesting for further analysis, [17]. The converter chain and its control system has been analysed [11, 17, 18, 19]. However, to the best of the author's knowledge,

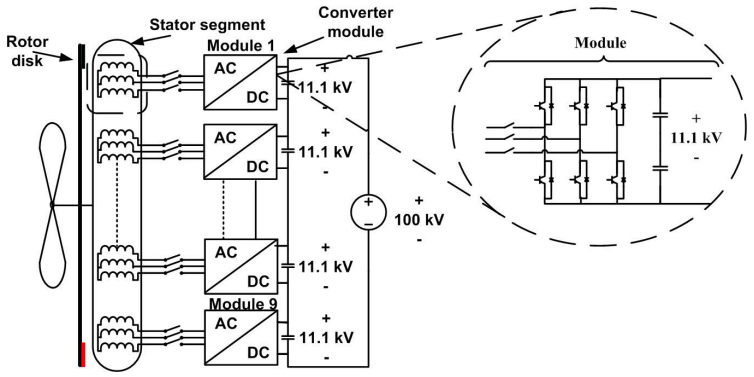

Fig. 1. Principal overview of the analysed transformerless generator/converter concept with converter module details (to the right).

only [11] has presented experimental results verifying control of such a converter topology. These results are limited to two converter modules connected to one generator unit each, mounted on the same shaft. This work makes use of a converter chain with several modules operating on a floating voltage potential, and the operation of such a configuration is necessary to verify. Additionally, the behaviour and modelling of the special, segmented generator must be validated. Therefore, the experimental verification presented here was performed with three converter modules in series (one floating) connected to a prototype of the segmented generator. The experimental results are compared to simulations in EMTDC/PSCAD for validation of the simulation modelling approach.

2. System configuration of the transformerless wind turbine concept

2.1. The generator

The Axial Flux, IronLess stator, PMSG (AF-IL-PMSG), which this work is based on, was initially designed for a low weight, 3-phase medium voltage system in a direct drive offshore wind turbine. A modular machine is obtained by splitting the stator winding into N 3-phase groups, Fig.1. These N segments are both physically and electrically separated in the stator.

The ironless stator, together with the concentrated coils, gives magnetic coupling between the machine segments. Consequently, the generator segments can be assumed to behave as independent machines mounted on a common shaft. This simplifies the control system and system modelling for simulations [17].

To the best of the authors knowledge, no former generator design has been able to handle high voltages in the stator without compromising the weight. However, in [20], a solution for high voltage machine insulation is proposed. A simplified view on the principle is to divide the electric field in the stator into DC-levels with superimposed AC-field. The turn-turn insulation in each segment is only related to the amplitude of the superimposed AC-field, while the insulation requirement between segment and ground is set by the DC-field, which is controlled by an electrostatic screen in the segment. Therefore, an efficient machine insulation design demands a limited amplitude on the AC-voltage. To achieve this, a DC-source split in many levels with balanced module voltages will yield the best overall results. [20] allows, with sufficient voltage levels, the application of standard machine winding insulation even for a 100 kV_{dc} output. This results in a more compact machine design than the cabled stator [15].

2.2. Converter topology

The modular series connected converter [11] in this work is based on 3-phase Voltage Source Converter (VSC)-modules series connected on the DC-side for synthesizing HVDC directly from the converter. The

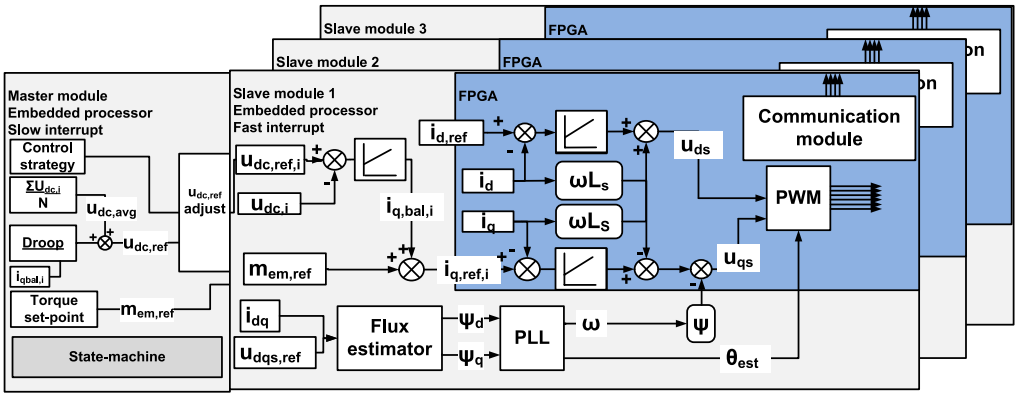

Fig. 2. Control system structure divided in master control and module control with indication of the main division between embedded processor and FPGA implementation for realization of the control modules in the experimental set-up.

AC-side of each module is connected to one generator segment. This results in the partitioning of the HVDC-voltage as required for the generator insulation.

An estimate in [20] indicated that N=9 modules results in a good trade-off between complexity and insulation thickness, and consequently machine weight. This results in an 11.1 *kV* DC-bus in the VSCs. Therefore, multilevel converter modules would be beneficial, both for converter and generator design. Based on N=9, [21] propose to use 5-level modular multilevel converters (MMC) [22]. However, it was shown that the choice of VSC-topology for the modules do not affect the overall system behaviour. Therefore, the standard 2-level converter (Fig.1) is used for simplified generator/converter system analysis in this work. A full system optimization which includes the converter voltages, robustness and complexity could end up with different N, bus voltages and converter topologies. Such an optimization is outside the scope of this work.

2.3. Control system

A suitable control system (Fig.2) which complies with the basic demands of the system was first proposed by [11], and further analysed and developed in [17, 18, 19]. The principle is a modular control system where each VSC can be controlled independently of the others, without synchronisation between the modules. In the main turbine control unit, the torque, DC-voltage reference and state-machine is controlled. Also eventual other top-level control strategies and fault tolerant control modes can be implemented here. The interface to the module controllers is through $m_{em,ref}$ and $u_{dc,ref}$. Each slave controller is equivalent to that of a standard 3-phase motor drive with Pulse Width Modulation (PWM), current control and sensorless rotor position tracking, Fig.2. In addition, a DC-bus voltage controller is included. The controller is under normal operation used for balancing the DC-bus voltages. However, by altering the set-point for $U_{dc,ref}$ for the different converter modules, other control strategies can be implemented, based on the operating conditions in the system. The DC-voltage control interacts with the system through an addition to the torque reference. This DC-bus voltage controller is included in each of the modules, to preserve a modular approach. However, for the N controllers there are only N-1 degrees of freedom in the system. Therefore, a droop control is added in the main control. The droop control is based on the sum of the DC-bus voltage controller outputs.

3. Experimental verification

3.1. Introduction to the experimental verification

The experimental results presented here verifies the modular series connected converter with modules operating on floating potential. Also, the control system and operation of the modular converter connected to

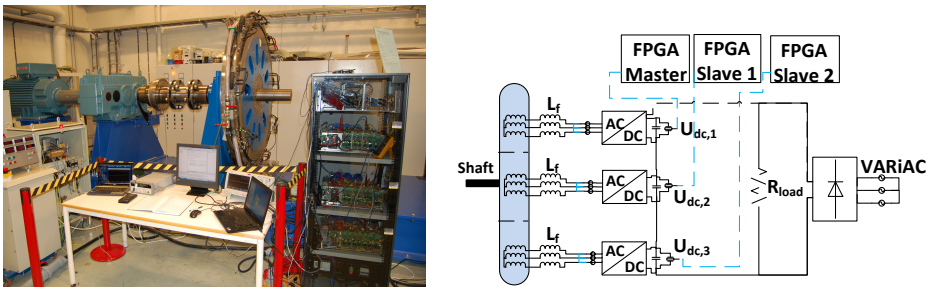

(a) (b)

Fig. 3. a)The 45 kW laboratory set-up, with drive machine, gear-box, AF-IL-PMSG with 3 segments, rack with modular converter + digital control system and control/monitoring computer.b) Simplified connection scheme of the set-up.

one physical generator unit with segmented stator is validated. The experimental results are compared to simulations to verify a simulation model built in EMTDC/PSCAD.

3.2. Description of laboratory set-up

A low voltage, 45 kW prototype of the AF-IL-PMSG, made by SmartMotor, is used in this work together with converter modules rated 20 kW each [23]. This prototype was originally made with a 3-phase stator winding, but was reconfigured to three electrically isolated segments. In the experimental work presented here, the generator prototype was de-rated in two ways: first, the nominal speed was reduced to 40 rpm due to limitations in the gear box. Second, the nominal current was limited to 35 A_{rms}, due to trouble with the stator water cooling. The 20 kW converters are standard, designed for laboratory use. Oversized semiconductors and an extensive interlock circuit with conservatively tuned protection functions gives robustness against overload and control system errors. The interface between the converter unit and control circuit is logic signals from the PWM-modulator.

The control system, Fig.2, was realized on controller boards based on FPGAs with embedded processor core [24]. Three boards were used, one for each VSC-module, with a 32-bit asynchronous master/slave data communication. The main controller was implemented in one of the three FPGA-boards which served as master card.

The HVDC-insulation technology was not implemented in this generator prototype. It is, however, not directly relevant for the operation and control of the VSC-chain. Nor will it affect the operation of the axial flux generator seen from a control perspective. Therefore, this does not limit the results of the verification presented in this paper.

As DC-grid model, a load resistor and a diode bridge was used. The diode bridge maintained a no-load voltage of 0.9 pu in the DC-link.

Table 2. Laboratory set-up essential parameters

Machine parameter	Value		Converter Parameter	Value
AF-IL-PMSG (SmartMotor) rated power	45 kW		VSC-module rated power	20 kW
Generator rated voltage, 3-phase	240 V_{ll}		VSC-module switching frequency f_{sw}	2 kHz
Generator rated current with water cooling	110 A_{rms}		VSC-module bus capacitor C_{bus}	3300 μF
Generator rated current without water cooling	35 A_{rms}		Totalt DC-link voltage $U_{dc,tot}$	225 V
Generator rated speed	74 rpm			
Max generator speed due to gearbox	40 rpm			
Pole pairs	24			
Number of stator segments	3			

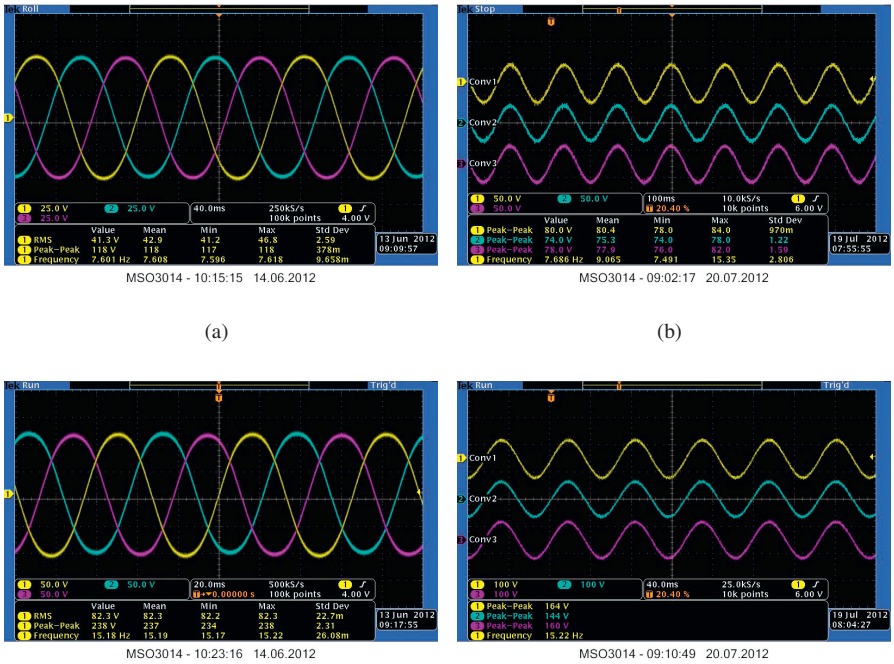

Fig. 4. No load voltages a) Phase voltages, 20 rpm, standard 3-phase winding configuration b)Line voltage, U_{ab} at 20 rpm, segmented stator with 3 winding groups c) Phase voltages, 40 rpm, standard 3-phase winding configuration d)Line voltage, U_{ab} at 40 rpm, segmented stator with 3 winding groups (Ch.1-3: Generator voltage)

3.3. No-load operation and verification of decoupled generator segments

The first step of the laboratory experiment was to verify the no-load behaviour with a segmented stator windings.In Fig.4(a), the 3-phase version is shown for 20 rpm, and in Fig.4(b) the segmented version. By comparing the two figures, it can be observed that the frequency is preserved. The measured phase voltage in the standard configuration corresponds well with the lowest measured line voltage in the three segment connection. At 20 rpm, the deviation from the lowest to the highest excitation is 7.3 %. At 40 rpm, it is 13.9 %. The cause of this is rotor skew with respect to the stator, and eccentricity in the rotor disk, Fig.4(b) and Fig.4(d).

To verify the absence of magnetic coupling between the generator segments, two generator segments were loaded while the third module was disconnected. The DC-link was not precharged, and the two connected converters were used as diode rectifiers. The generator speed was 20 rpm. A step in the resistive load was then applied, Fig.5. This load step was applied at 500 ms, and can be observed as an increase in the phase current of module 1 and the increased ripple in $U_{dc,1}$ and $U_{dc,2}$. If there was a magnetic coupling, this step should have resulted in a response in the no-load phase voltage of segment 3. However, the phase voltage remains the same, and it can be concluded that the magnetic coupling between the stator segments is negligible.

3.4. Simulation model for comparison with the experimental results

The generator/converter was simulated using EMTDC/PSCAD. One synchronous generator model with fixed excitation was used for modelling each stator segment [18]. The rated voltage of the generator pro-

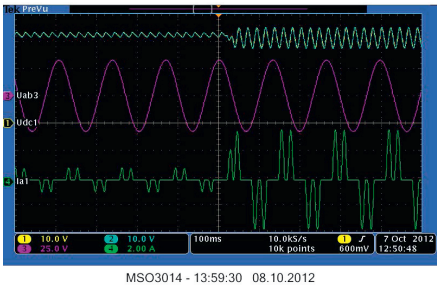

Fig. 5. Response to a step in the resistive DC-load, with two stator segments connected to converter modules operated as passive rectifiers -diode bridges, while the third segment was disconnected. Ch.1 and 2 displays the DC-bus voltages of the two connected modules, ch.3 the induced voltage of the disconnected segment and Ch.4 the current of module 1(Ch.1: $U_{dc,1}$, Ch.2: $U_{dc,2}$), Ch.3: $U_{ab,3}$, Ch.4: I_{load})

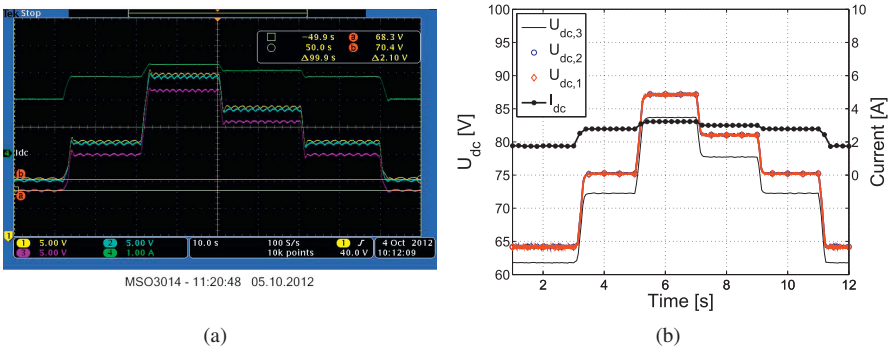

(a) (b)

Fig. 6. Response constant torque/speed ramp with current controlled converter modules (without the DC-bus voltage control activated). a) Voltage measurement of the initial voltage deviation = 2.1 V. (Ch.1: $U_{dc,1}$, Ch.2: $U_{dc,2}$, Ch.3: $U_{dc,3}$, Ch.4: I_{load}) b) Corresponding simulation.

totype was used, and the excitation was adjusted to comply with the actual induced voltages (according to Fig.4(b) and 4(d).

The charging circuit was considered as an ideal diode bridge and an AC-voltage source. Finally, the drive machine and shaft was assumed stiff, and modelled as a speed input with ramp limiter.

3.5. Generator/converter without DC-bus voltage control - current control mode

In Fig.6(a), the generator speed is ramped up from 20 to 40 rpm, while the torque is maintained constant at 0.1 pu. A small increase in the DC-bus voltage imbalance can be observed from the initial to the maximum loading, 2.1 V (3.8 % of average DC-bus voltage) to 2.8 V at the highest speed. The simulated cases show the same behaviour, Fig.6(b). Note that the time scale is 1/10 in the simulations, to reduce the computational effort.

The oscillations in the uncontrolled DC-bus voltage have a frequency which corresponds to the rotational speed of the generator. These oscillations are due to mechanical displacements in the generator, and are partly the explanation of the large differences in no-load voltages, Fig.4(d). These variations in excitation of the stator were not included in the simulation model.

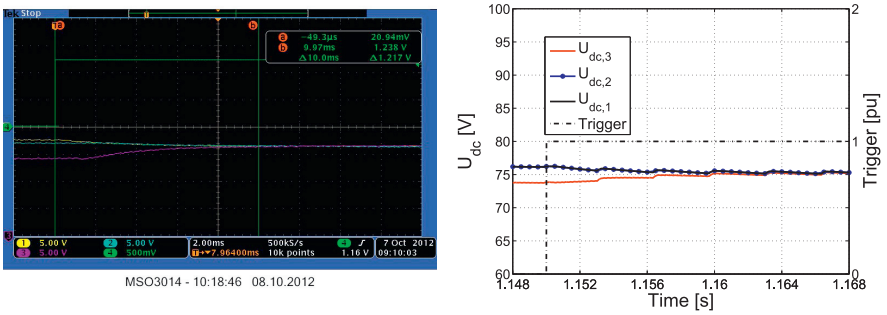

(a) (b)

Fig. 7. Response to the transition from current control mode to DC-bus voltage balance control. a)Laboratory measurement. Channel 1-3 are voltages, while channel 4 is the activation signal, output for exact trigging. (Ch.1: $U_{dc,1}$, Ch.2: $U_{dc,2}$, Ch.3: $U_{dc,3}$, Ch.4: Trigger signal) b) Corresponding simulation.

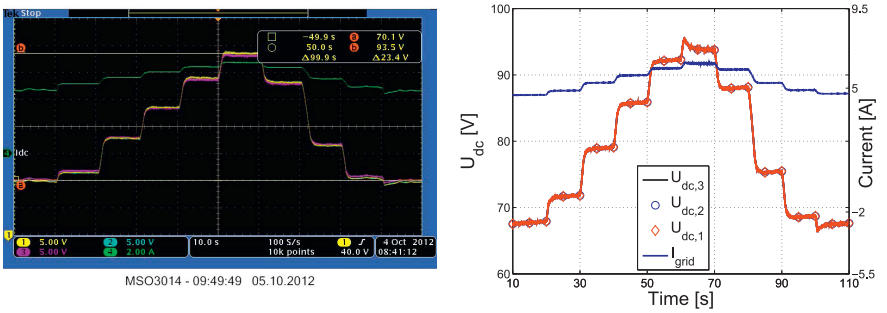

(a) (b)

Fig. 8. Torque ramp-constant speed operation a) Laboratory results. (Ch.1: $U_{dc,1}$, Ch.2: $U_{dc,2}$, Ch.3: $U_{dc,3}$, Ch.4: I_{load}) b) Corresponding simulation

3.6. DC-bus voltage control response

Fig.7(a) shows the response in the generator/converter system during the transition from current control to DC-voltage balance control. The time to achieve balance is approximately 8 ms, without controller overshoot, at a rotational speed of 20 rpm and torque reference of 0.04 pu, Fig.7(a). The corresponding simulation is presented in Fig.7(b). There is a good agreement with the experimental data, although the response time is slightly longer in the simulations.

3.7. DC-voltage control without droop control

In Fig.8(a), the issue with an overdetermined system is illustrated by ramping up and down of the turbine torque under constant speed without the droop control activated. The second step (10 s -20 s) has the same torque set-point as the second last (80 s - 90 s). However, the resulting generator loading differs, which can be seen as different DC-bus voltages. As a result, the actual operating point of the generator/converter system ends up in a different state than expected, and is not consistent. Fig.8(b) presents the same phenomena in the simulations, with good correspondence. There is a small difference in starting point, originating from an offset in the measurement acquisition in the AD-converter.

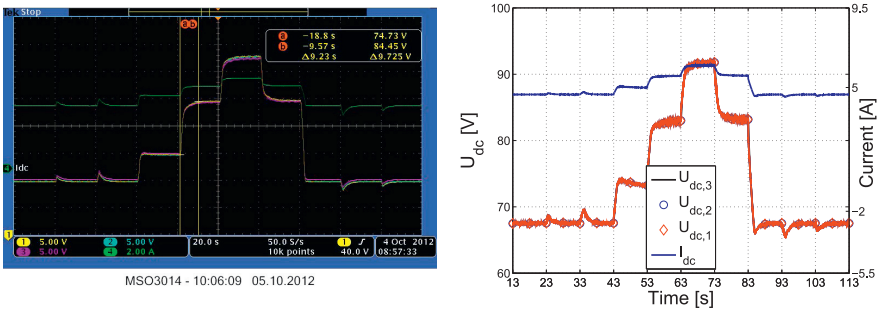

(a) (b)

Fig. 9. a)Torque ramp with droop constant = 0.1. Until t=30 s, and from t=90 s, the DC-bus reference set-point is restricted to maintain a minimum load voltage. In between, the set-point is based on a balanced DC-bus voltage strategy, and the droop control ensures that the operation point corresponds to the expected.(Ch.1: $U_{dc,1}$, Ch.2: $U_{dc,2}$, Ch.3: $U_{dc,3}$, Ch.4: I_{load}) b) Corresponding simulation.

3.8. DC-bus voltage control with droop

With the droop control implemented, the steady state operating point of the system does only depend on the main torque reference, rotational speed of the turbine and DC-load. By comparing the experimental results in Fig.9(a) with Sec.3.7, the effect of the droop can be observed: With the droop, the correspondence between set-point and operating point is consistent. The initial 30 seconds of the time-series, the torque set-point results in a lower power than required to maintain the DC-link voltage above the minimum. This results in the set-point for the DC-bus references of being constant, and the DC-bus control acts to compensate (inject more power to the DC-link). When the torque is increased, the DC-bus control does not need to compensate equally much, and the droop control forces the DC-reference set-point back. Since the droop control is slower than the torque control, this process is observed as a transient in the DC-bus voltage for each increase in torque reference. At t=30 seconds, the torque set-point results in higher power than the minimum required to maintain the load voltage above the lower limit, and the DC-voltage set-point is now generated for maintaining balanced module voltages.

4. Conclusion and further work

This paper has presented the experimental verification process of a modular, series connected voltage source converter suitable for a transformerless offshore wind turbine drive. The key verification point was the validity of a modular control synthesis approach. First, the machine modelling approach was verified. Then, current control of the generator/converter system was verified. Finally, the DC-bus voltage control design approach was validated, with and without DC-voltage droop. From the results, the necessity of a droop control to preserve control of the system was observed.

The experimental data were compared to simulation results to validate the approach being used when implementing the system model in EMTDC/PSCAD. Generally, an acceptable accordance between the measured and simulated waveforms was found, although there were some small deviations which can be ascribed to the detail level of the simulation model.

Further work includes converter fault scenarios, DC-grid transients and insulation system [20] verification.

Acknowledgements

This work has been co-founded by The Norwegian Research Centre for Offshore Wind Technology, NOWITECH. The authors also acknowledge the support from SmartMotor AS for the possibility to use the ironless, Axial

Flux-PMSG prototype for the experiments.

References

[1] P. Jamieson, Upscaling of Wind Turbine Systems, John Wiley & Sons, Ltd, 2011, pp. 75–104. doi:10.1002/9781119975441.ch4. URL http://dx.doi.org/10.1002/9781119975441.ch4

[2] O. Dalhaug, P. Berthelsen, T. Kvamsdal, L. Frøyd, S. Gjerde, Z. Zhang, K. Cox, E. Van Buren, D. Zwick, Specification of the NOWITECH 10 MW Reference Wind Turbine, Tech. rep., Norwegian Research Centre for Offshore Wind Technology, Trondheim, Norway (2012).

[3] N. Fischaux, J. Wilkes, F. Hulle, A. Cronin, Oceans of Opportunity - Harnessing Europes largest domestic energy resource, Tech. rep., European Wind Energy Association (EWEA) (Sept. 2009).

[4] Z. Zhang, A. Matveev, S. Ovrebo, R. Nilssen, A. Nysveen, State of the Art in Generator Technology for Offshore Wind Energy Conversion Systems, in: Electric Machines Drives Conference (IEMDC), 2011 IEEE International, 2011, pp. 1131 –1136. doi:10.1109/IEMDC.2011.5994760.

[5] C. Ng, M. Parker, L. Ran, P. Tavner, J. Bumby, E. Spooner, A Multilevel Modular Converter for a Large, Light Weight Wind Turbine Generator, Power Electronics, IEEE Transactions on 23 (3) (2008) 1062 –1074. doi:10.1109/TPEL.2008.921191.

[6] M. Parker, C. Ng, L. Ran, P. Tavner, E. Spooner, Power Control of Direct Drive Wind Turbine with Simplified Conversion Stage Transformerless Grid Interface, in: Universities Power Engineering Conference, 2006. UPEC '06. Proceedings of the 41st International, Vol. 1, 2006, pp. 65 –68. doi:10.1109/UPEC.2006.367716.

[7] X. Yuan, Y. Li, J. Chai, M. Ma, A Modular Direct-Drive Permanent Magnet Wind Generator System eliminating the Grid-side Transformer, in: Power Electronics and Applications, 2009. EPE '09. 13th European Conference on, 2009, pp. 1 –7.

[8] X. Yuan, Y. Li, J. Chai, A Transformerless Modular Permanent Magnet Wind Generator System with Minimum Generator Coils, in: Applied Power Electronics Conference and Exposition (APEC), 2010 Twenty-Fifth Annual IEEE, 2010, pp. 2104 –2110. doi:10.1109/APEC.2010.5433526.

[9] X. Yuan, J. Chai, Y. Li, A Transformer-Less High-Power Converter for Large Permanent Magnet Wind Generator Systems, Sustainable Energy, IEEE Transactions on 3 (3) (2012) 318 –329. doi:10.1109/TSTE.2012.2184806.

[10] F. Deng, Z. Chen, A New Structure Based on Cascaded Multilevel Converter for Variable Speed Wind Turbine, in: IECON 2010 - 36th Annual Conference on IEEE Industrial Electronics Society, 2010, pp. 3167 –3172. doi:10.1109/IECON.2010.5674975.

[11] M. Carmeli, F. Castelli-Dezza, G. Marchegiani, M. Mauri, D. Rosati, Design and analysis of a Medium Voltage DC Wind Farm with a Transformer-Less Wind Turbine Generator, in: Electrical Machines (ICEM), 2010 XIX International Conference on, 2010, pp. 1 –6. doi:10.1109/ICELMACH.2010.5607878.

[12] P. Maibach, M. Eichler, P. Steimer, Energy System,US2009/0212568 A1 (2009).

[13] M. Garces, A.and Molinas, High Frequency Wind Energy Conversion from the Ocean, in: Power Electronics Conference (IPEC), 2010 International, 2010, pp. 2056 –2061. doi:10.1109/IPEC.2010.5543443.

[14] A. Mogstad, M. Molinas, P. Olsen, R. Nilsen, A Power Conversion System for Offshore Wind Parks, in: Industrial Electronics, 2008. IECON 2008. 34th Annual Conference of IEEE, 2008, pp. 2106 –2112. doi:10.1109/IECON.2008.4758282.

[15] M. Dahgren, H. Frank, M. Leijon, F. Owman, L. Walfridsson, WindformerTM: Wind power goes large-scale, in: ABB Review, No.3, 2000.

[16] R. O'Donnell, N. Schofield, A. Smith, J. Cullen, Design Concepts for High-Voltage Variable-Capacitance DC Generators, Industry Applications, IEEE Transactions on 45 (5) (2009) 1778 –1784. doi:10.1109/TIA.2009.2027545.

[17] S. Gjerde, T. Undeland, Power Conversion System for Transformer-Less Offshore Wind Turbine, in: Power Electronics and Applications (EPE 2011), Proceedings of the 2011-14th European Conference on, 2011, pp. 1 –10.

[18] S. Gjerde, T. Undeland, A Modular Series Connected Converter for a 10 MW, 36 kV, Transformer-Less Offshore Wind Power Generator Drive, Energy Procedia 24 (0) (2012) 68 – 75, selected papers from Deep Sea Offshore Wind R&D Conference, Trondheim, Norway, 19-20 January 2012. doi:10.1016/j.egypro.2012.06.088.
URL http://www.sciencedirect.com/science/article/pii/S1876610212011289

[19] S. Gjerde, P. K. Olsen, T. Undeland, A Transformerless Generator-Converter Concept making feasible a 100 kV Low Weight Offshore Wind Turbine Part II - The converter, in: Energy Conversion Congress and Exposition (ECCE), 2012 IEEE, 2012, pp. 253 –260. doi:10.1109/ECCE.2012.6342815.

[20] P. K. Olsen, S. Gjerde, R. M. Nilssen, J. Hoelto, S. Hvidsten, A Transformerless Generator-Converter Concept making feasible a 100 kV Light Weight Offshore Wind Turbine: Part I - The generator, in: Energy Conversion Congress and Exposition (ECCE), 2012 IEEE, 2012, pp. 247 –252. doi:10.1109/ECCE.2012.6342816.

[21] T. M. Iversen, S. Gjerde, T. Undeland, Multilevel Converters for a 10 MW, 100 kV Transformer-less Offshore Wind Generator system, in: EPE Joint Wind Energy and T&D Chapters Seminar - Aalborg, Denmark, 2012.

[22] A. Lesnicar, R. Marquardt, An Innovative Modular Multilevel Converter Topology Suitable for a Wide Power Range, in: Power Tech Conference Proceedings, 2003 IEEE Bologna, Vol. 3, 2003, p. 6 pp. Vol.3. doi:10.1109/PTC.2003.1304403.

[23] H. Kolstad, K. Ljøkelsøy, Sintef report An 01.12.12: 20 kW IGBT omformer. Beskrivelse. 3.utgave (Norwegian), Tech. rep., Sintef Energy (2002).

[24] K. Ljøkelsøy, FPGA based processor board for control of power electronics converters, Tech. rep., SINTEF Energy Research (2008).